Experimental characterization of Pombalino "frontal" wall cyclic behaviour

Ana Maria Gonçalves, Joao Gomes Ferreira, Luis Guerreiro, Fernando Branco
Instituto Superior Técnico, Lisboa, Portugal

SUMMARY:
After the large destruction of Lisbon due to the 1755 earthquake, the city had to be almost completely rebuilt. The innovative "pombaline" buildings were then developed. This type of building is characterized by its structural interior "frontal" walls in elevated floors, constituted by a timber frame with vertical and horizontal elements, braced with diagonal elements (Saint Andrew's crosses) with masonry infill.
This paper describes an experimental campaign to assess the in-plane cyclic behaviour of "frontal" walls and to evaluate the effect of its different components (timber frame, masonry). Experimental characterization of the in-plane behaviour was carried out by static cyclic shear testing with controlled displacements. The loading protocol used was the CUREE for ordinary ground motions. The hysteretic behaviour main parameters of such walls subjected to cyclic loading were computed namely the initial stiffness, ductility, energy dissipation capacity and viscous damping.

Keywords: "Pombaline" buildings, cyclic loading tests, earthquake

1. INTRODUCTION

Timber framed wall buildings are seen all over Europe, especially in seismic regions, given its adequacy to resist earthquake (Diskaya, 2007; Dogangun, *et al*. 2006; Gulkan, 2004; Langenbach, 2007; Makarios and Demosthenous, 2006, Redondo, *et al.* 2003). The "pombaline" buildings, named after the Marquis of Pombal, in particular, present a structure with maximum of four storeys, with arcades at the ground floor and masonry facade walls, and internal timber framed masonry walls, called "frontais". These walls, together with the floors' timber beams, form the 3-D cage ("gaiola", in Portuguese) that constitutes the seismic resistant structure (Figure 1). The Marquis of Pombal ordered their construction after the 1755 earthquake that destroyed Lisbon, aiming at providing the city with seismic resistant buildings (Ferreira, *et al.* 2012).

Figure 1. Frontal wall in "pombalino" Building (Gonçalves, *et al* 2011)

Though the "pombaline" structure has a good seismic behaviour, after more than 250 years these

buildings need rehabilitation works because of their degradation, the inadequate interventions they have been subjected to (such as adding storeys, modifying structural elements or changing the functionality of the building) and because the new codes more demanding rules for earthquake resistance.

It was the limited knowledge on the whole behaviour of the "pombaline" cage system, and particularly on frontal wall´s behaviour, that motivated the experimental programme presented in this paper.

2. EXPERIMENTAL PROGRAMME

The objective of the experimental work developed and presented herein is to obtain the hysteresis behaviour of the "frontal" walls through static cyclic shear testing with controlled displacements. Simple timber frames (without masonry infill) were also tested to assess the contribution of these frames to the whole behaviour of the timber-masonry wall.

2.1. Objectives

The experimental work on frontal walls comprised two parts. The first parte consisted of an experimental campaign to assess the in-plane seismic behaviour of "frontal" walls and to evaluate the effect of its components (timber frame, masonry) (Figure 2). The second parte aimed at evaluating the adequacy and efficacy of three proposed seismic rehabilitation methods based on buckling restrained damping braces, steel plate reinforcement on timber elements connections and reinforced plaster. In this paper only the first part an experimental campaign will be presented.

2.2. Test specimens

The tested models consist of four modules, i.e., a module with four Saint Andrew's crosses. The tests were performed on two modules of timber Saint Andrew's crosses without masonry infill, referred to as timber frames, and two identical modules with masonry infill, referred to as masonry walls (Fig. 2).

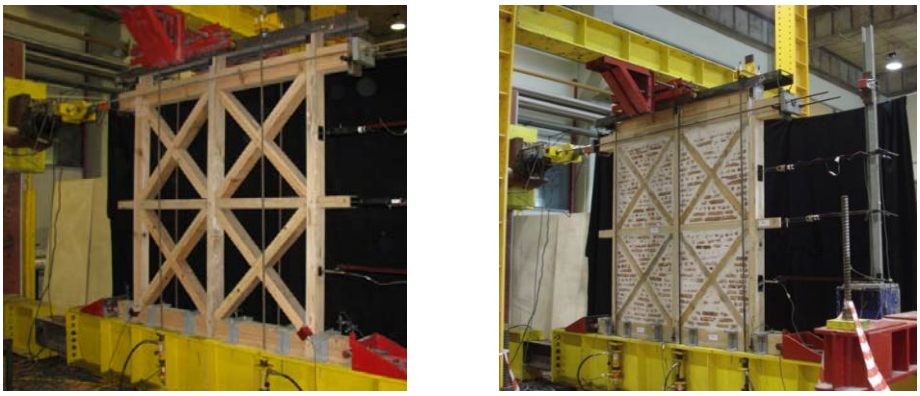

a)Timber frame (TF) b) Masonry wall (MW)

Figure 2 . Experimental models.

Cross-having joints were used in the connections between vertical and horizontal timber elements and between the crossing diagonals. The connections between the diagonals and their end nodes were obtained by simply sawing at 45º. All connections were reinforced with iron nails. The wood used in that experimental study was stone pine. The wood sections were: 16x12 cm^2 and 8x12 cm^2. Figure 3 shows the size of the timber frame wall.

The choice of the type of masonry was very important since there are several types of infill, including mortar with bricks or mortar with tiles or even mortar mixed with small stones. In this study, mortars with bricks (Figure 4) were used. The masonry consists of bricks and cement-lime-sand mortar with a volume ratio of 1:2:6 (hydrated lime (air): portland cement 32.5 N : sand). Although ancient mortars

were solely composed of lime and sand, cement was added in these cases to ensure a faster cure. The drying time is two months.

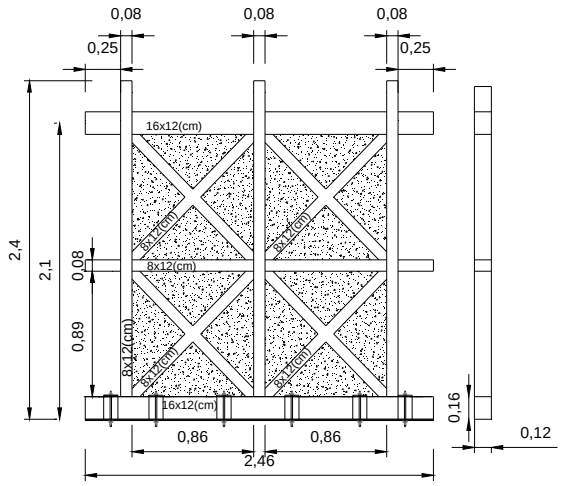

Figure 3. Models' dimensions (m)

Figure 4. Masonry wall fabrication

2.3. Experimental procedures

A series of quasi-static tests were performed in the reaction wall at the Laboratory of Structures and Strength of Materials of the Instituto Superior Técnico. The tests involved the application of horizontal and vertical load on the models. The walls were tested with the horizontal displacements applied at the top of the wall, using a 400 mm stroke actuator with a 1.000 kN capacity.

The wall was fully instrumented to measure the displacement at different points. The displacement transducers D1 to D4 measured the horizontal displacement on the wall at different heights, D5 to D7 measured the vertical lift of the vertical timber element in regard to the bottom wood beam, D8 and D9 measured the displacement in the diagonals. The load imposed by the actuator was also measured with a load cell, as well as the tension in the vertical cables used to impose the vertical load.
The general layout of the equipment is shown in Figure 5.

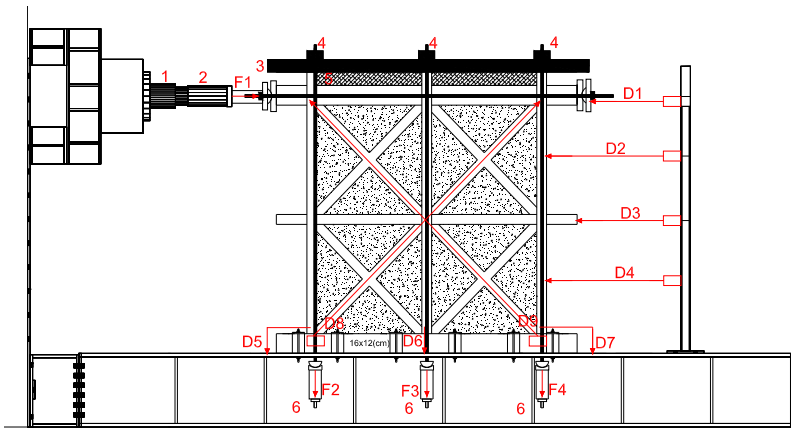

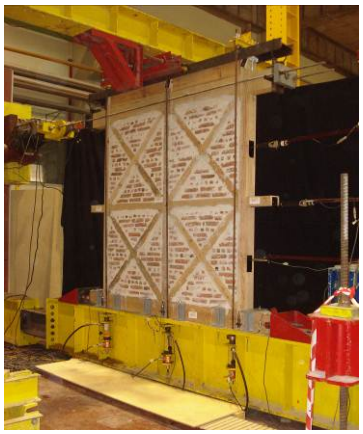

Legend: 1) Actuator; 2) Load Cell; 3) Beam Charge distribution; 4) Road of prestressing; 5) Wooden beam 6) hydraulic jacks; D1 to D8) linear variable differential transducer

Figure 5. Test set-up

To prevent the masonry wall from having rocking movement, the bottom wooden beam was bolted to a base steel beam with six fixation points. The out of the plane motions was prevented with lateral

rollers at the top.

The test procedure consisted of imposing a horizontal displacement at the top. A constant vertical load was transmitted at the top of the elements to simulate gravity loads with six steel cables tensioned with hydraulic jacks. The vertical loading to impose on the test structure was determined based on EN 1991-1 (CEN, 2002) and is given by equation 1. It was considered that the wall was placed at the first floor of a three story building plus ground floor. The area of influence of the walls was considered to be of 5 m^2. The total vertical load applied to the masonry wall was 30 kN/m.

$$S_d = SW + 0.3 \times LL \quad (1)$$

Where S_d is the vertical loding, SW is the self-weight, LL is the live load.

2.4. Loading protocol definition

Experimental characterization of the in-plane behaviour was carried out by static cyclic shear testing with controlled displacements, as referred. The loading protocol used was the CUREE (Krawinkler, 2000; EN 1015, 1999). This protocol consists of cyclic displacement sequences increasing in amplitude throughout the test, each segment consisting of a primary cycle, with the amplitude defined as a multiple of the reference displacement, followed by a series of cycles with amplitude equal to 75% of the primary cycle (Table 2.1).

Table 2.1. History of displacement

Segment	Nº of cycles	Amplitude in the primary cycle (%)×Δ
1	6	5% ×Δ
2	7	7.5% ×Δ
3	7	10% ×Δ
4	4	20% ×Δ
5	4	30% ×Δ
6	3	40% ×Δ
7	3	70% ×Δ
8	3	100% ×Δ
9	3	(100% + 100% ×α) ×Δ
10	3	(100% + 2×100% ×α) ×Δ

Legend: Δ - reference displacement

The reference displacement was 90 mm, corresponding to the maximum displacement obtained at IST experimental tests (Meireles, 2010).

3. RESULTS

3.1. Timber Frames (TF)

The load-displacement diagrams obtained for the timber frames (TF) is shown in Figure 6. The cyclic displacements were imposed until submitting the walls to rupture. An increase in the walls stiffness, occurring for displacement higher than 60 mm, was identified in the load-displacement diagrams. However, this boost in the wall stiffness is due to the increase of strength in the tensioned cables jacks, when they reach their limit course and start to operate as tie rods. Due to this behaviour, these values cannot be taken into account for the characterization of the walls. The analysis is limited to a range of ± 55 mm displacements, which results in a 2.6% drift.

The hysteretic behaviour of the “frontal” walls subjected to cyclic loading is characterized by nonlinear behaviour with a high ductility response. The maxim strength is 30 kN for the timber frame walls, measured at the displacement of 55 mm (2.6% drift).

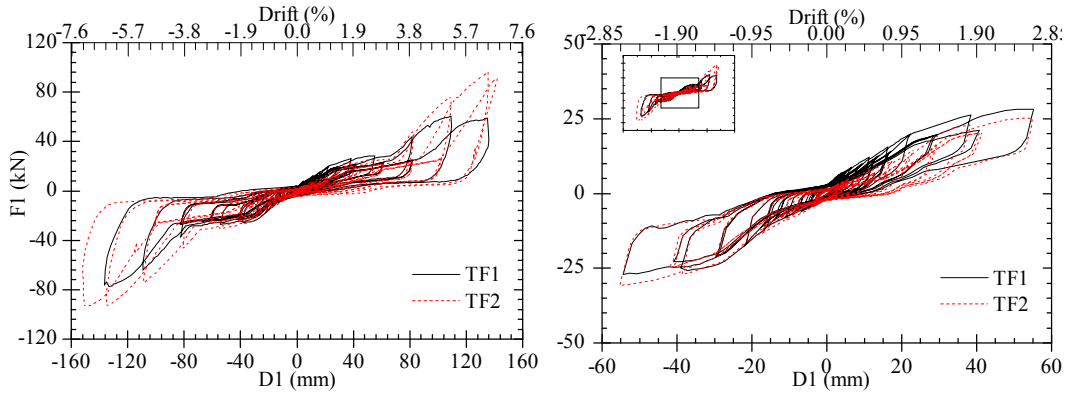

Figure 6. Force-Displacement curves of timber frames

As shown in figure 7, in the first cycles the timber frame walls present practically bilinear behaviour, up to approximately 10 kN and 12 mm (0.5% drift). As displacement increments, a number of effects such as cracking and plasticization or degradation of stiffness became more visible.

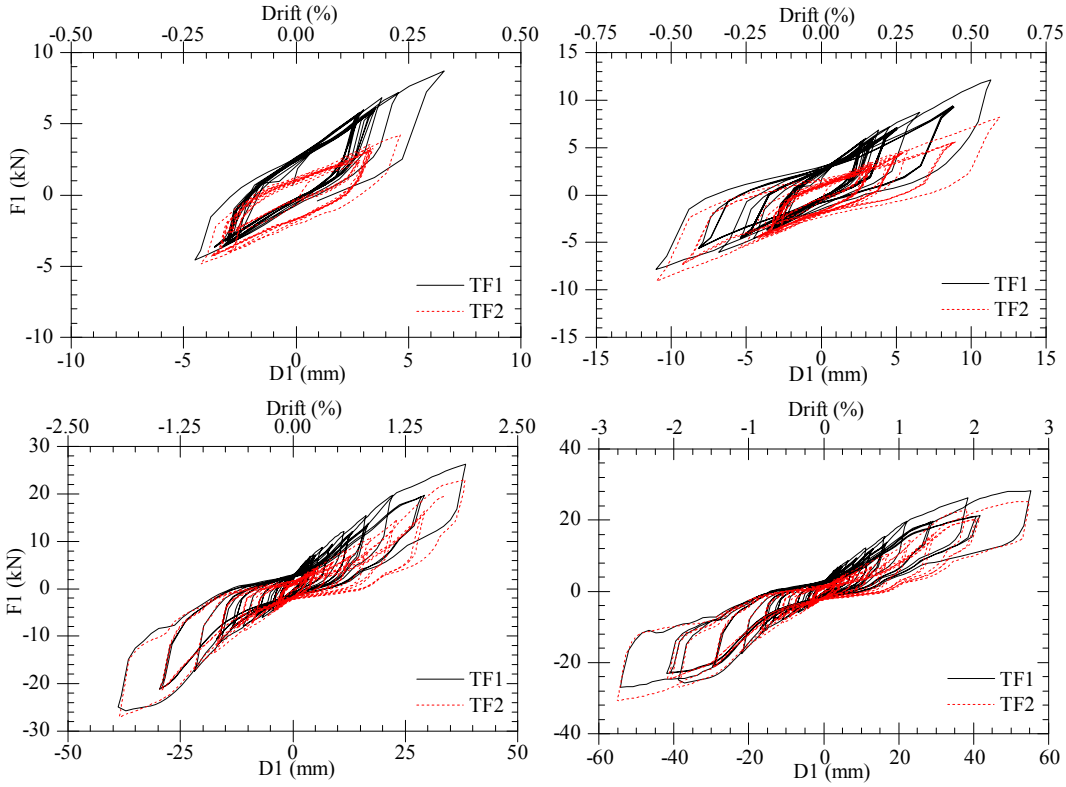

Figure 7. Force-displacement curves of timber frames

The locus of extremities of the load-displacement hysteresis loops are envelope curves. The envelope curve contains the peak loads of the first cycle of each segment of the cyclic loading. Wall displacement in the positive direction produces a positive envelope curve; the negative wall displacement produces a negative envelope curve .

According to ISO 21581 (2009), the first, second and third envelope curves for the cyclic tests shall be established by connecting the points of maximum load in the hysteresis plot in each displacement level in the first, second and third reversed cycles, respectively (Figure 8).

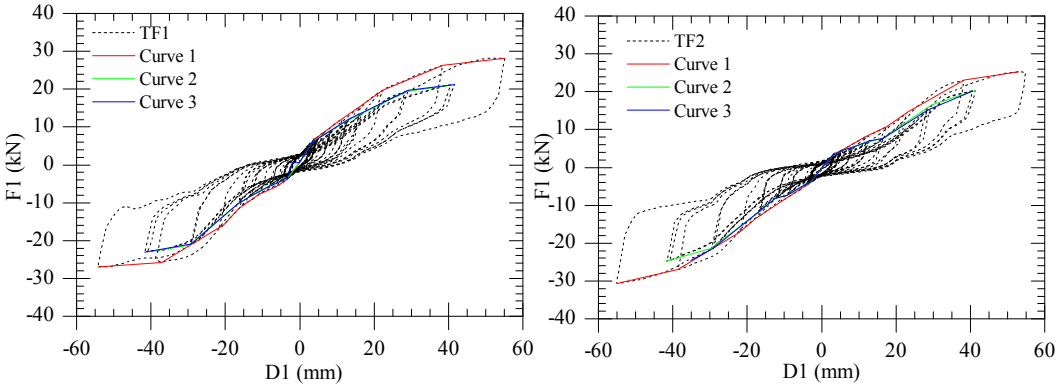

Figure 8. Force-displacement envelope curve

Properties such as stiffness, yield displacement, ductility and impairment of strength can be determined from the envelope curves according to the definitions adopted.
Stiffness may be calculated by equation 2 for the first, second and third envelope curves of the cyclic test specimens. Parameters $\nu_{40\%Fmax}$ and $\nu_{10\%Fmax}$ in equation (2) are the displacement values obtained at 40% and 10% of maximum load (F_{max}), respectively, for the envelope curves.

$$K = \frac{0.3 \times F_{max}}{\upsilon_{40\%F_{max}} - \upsilon_{10\%F_{max}}} \tag{2}$$

Accordingly the stiffness of the wall was estimated in 694 kN/m in the TF1 and 526 kN/m in the TF2 (average of three curves). This difference could be related with the behaviour of timber connections (Table 3.1).

Table 3.1. Wall stiffness

TF1	F_{max} (kN)	F_{min} (kN)	$\lvert F_{ave}$ (kN)$\rvert$	$\nu_{40\%Fmax}$ (mm)	$\nu_{40\%Fmin}$ (mm)	$\nu_{40\%Fave}$ (mm)	$\nu_{10\%Fmax}$ (mm)	$\nu_{10\%\ Fmin}$ (mm)	$\nu_{10\%\ Fave}$ (mm)	K (kN/m)
1ª curve	28.2	-27.0	27.6	12.3	-15.4	13.9	1.1	-2.8	2.0	696.0
2ª curve	21.1	-22.8	21.9	8.7	-13.7	11.2	0.9	-2.8	1.9	703.6
3ª curve	21.3	-21.0	21.2	8.5	-13.7	11.1	0.9	-2.8	1.9	686.6
TF2	F_{max} (kN)	F_{min} (kN)	$\lvert F_{ave}$ (kN)$\rvert$	$\nu_{40\%Fmax}$ (mm)	$\nu_{40\%Fmin}$ (mm)	$\nu_{40\%Fave}$ (mm)	$\nu_{10\%\ Fmax}$ (mm)	$\nu_{10\%\ Fmin}$ (mm)	$\nu_{10\%\ Fave}$ (mm)	K (kN/m)
1ª curve	25.2	-30.7	27.9	18.2	-14.3	16.2	2.7	-1.7	2.2	598.2
2ª curve	20.3	-24.7	22.5	18.1	-13.5	15.8	2.3	-1.7	2.0	488.7
3ª curve	20.1	-24.6	22.4	18.0	-13.2	15.6	2.2	-1.7	2.0	492.5

The energy dissipated in each cycle may be evaluated by calculating the area within the load-displacement curve in each cycle. Figure 9 and Table 3.2 show the behaviour of load - displacement of the walls along the cycles, where a decrease in damping with increasing imposed deformation can be observed. The damping coefficient for a given cycle may be estimated based on the following equation:

$$\zeta = \frac{E_d}{2\pi \times F_{max} \times d_{max}} \tag{3}$$

Dissipated energy, E_d, corresponds to the area of the graph formed by the cycle, F_{max} is the maximum force measured on the structure, and d_{max} is the maximum deformation in the structure.

The energy dissipation per cycle associated with the hysteretic behaviour of the wall was determined by measuring the area of the wider cycle in each stage of deformation in the force-displacement diagram. In table 3.2 the energy dissipated in cycles at different levels of deformation is presented. The increase in deformation leads to a higher increase in energy dissipation and less damping associated to damage in the wooden beams.

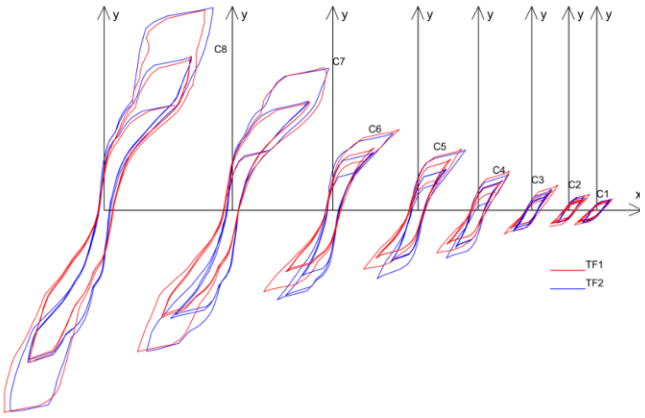

Figure 9. Energy dissipated in each cycle

Table 3.2. Energy dissipated and damping coefficient in each cycle

Cycle	TF1		TF2	
	E_d (kN/m2)	ζ (%)	E_d (kN/m)	ζ (%)
C1	19,75	19.3	15,38	20.3
C2	26,35	12.8	17,70	14.4
C3	48,74	13.5	32,40	18.0
C4	111,03	12.9	99,90	16.3
C5	181,15	8.4	181,87	12.2
C6	270,68	5.7	253,25	11.8
C7	721,08	11.3	641,67	11.6
C8	1138,03	11.7	1071,00	10.1

The load was increasing with the imposed displacement until the rupture of the diagonal associated with lateral instability. Figure 10 shows the failure modes of timber frames.

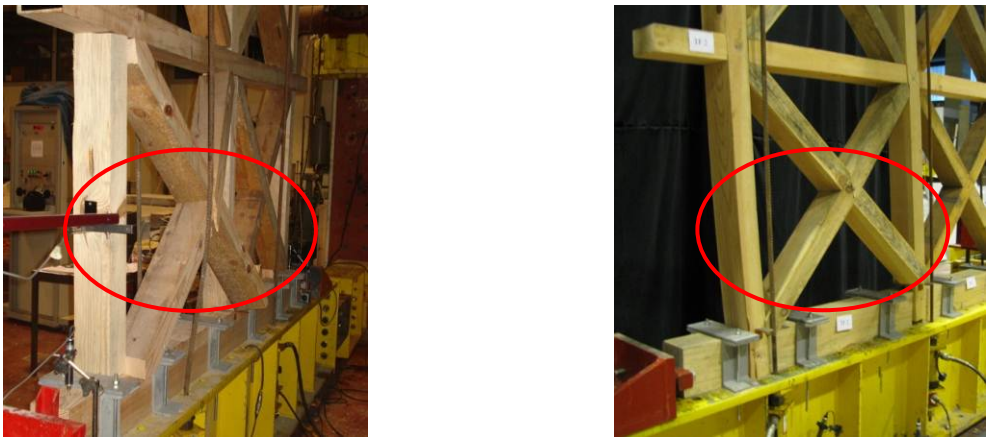

a) Failure by buckling of diagonal for TF1 b) Failure by buckling of diagonal for TF2

Figure 10. Failure mode of timber frames

3.2. Masonry walls

Two masonry walls, MW1 and MW2, constituted of a timber frame with masonry infill, were submitted to the same load cycles as the timbre frames (TF).
Figure 11 shows load-displacement diagrams, showing an increase in the wall stiffness for displacements higher than 60 mm due to the increase of load in the jacks, as occurred in the TF models. Due to this behaviour, these values cannot be taken into account for the characterization of the walls. The analysis is limited to a range of ± 55 mm displacements, which results in a 2.6% drift. The maximum strength within this cycles amplitude is 50 kN measured at the displacement of 55 mm which results in a 2.6% drift.

The results presented on figure 11 shows two distinct behaviours. In the first cycles the walls present practically linear behaviour, up to approximately 35 kN and 15 mm (0.7% drift). The small hysteresis loops in this phase are associated to gaps in the connections, which open and close according to the direction of the load. As displacement increments a number of effects that characterize the nonlinear behaviour become visible around 45 kN and 55mm of deformation which results in a 2.6% drift.

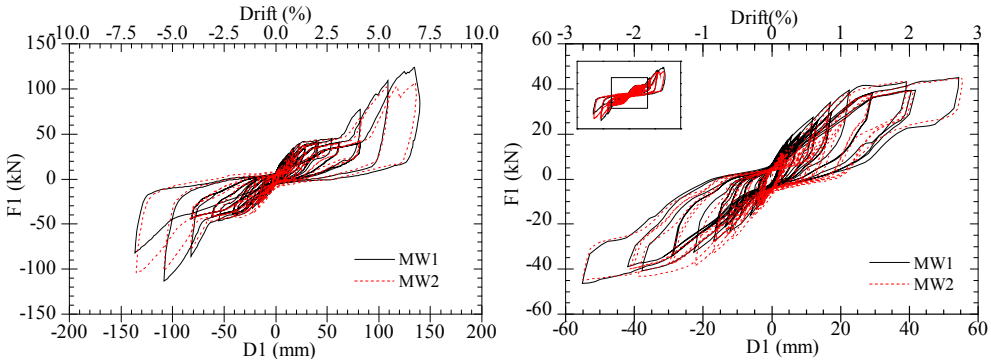

Figure 11. Force-displacement curves

The vertical lift of the bottom beam occurred during the wall test. Besides, a separation of the vertical timber beams from the bottom beam was observed as an effect of a rocking movement that was not eliminated, becoming more significant with the increase of the overall deformation (Figure 12).

Figure 12. Vertical lift of bottom beam and vertical member.

The curves shown in Figure 13 correspond to the evolution of hysteretic behaviour of the walls MW1 and MW2 that showed an identical behaviour. According to ISO/DIS 21581, stiffness properties are determined by the enveloping curves, with the equation 1. Figure 13 and Table 3.3 summarize the results obtained for the stiffness of the wall. Accordingly the stiffness of the wall was estimated in 2015 kN/m in the MW1 and 2000 kN/m in the MW2 (average of the three curves).

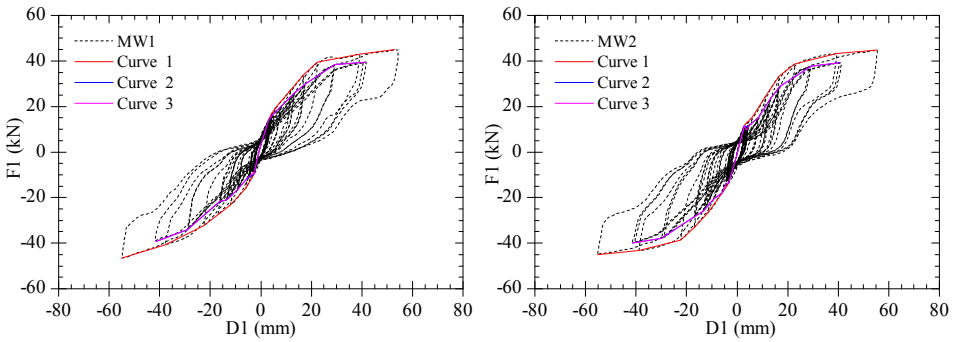

Figure 13. Force-Displacement curves

Table 3.3. Wall stiffness

MW1	F_{max} (kN)	F_{min} (kN)	$\lvert F_{ave}$ (kN)$\rvert$	$v_{40\%}F_{max}$ (mm)	$v_{40\%}F_{min}$ (mm)	$v_{40\%}$ (mm)	$v_{10\%}F_{max}$ (mm)	$v_{10\%}$ F_{min}(mm)	$v_{10\%}F_{ave}$ (mm)	k (kN/m)
1ª curve	45.1	-55.0	50.1	6.1	-9.1	7.6	0.1	-1.5	0.8	2209.4
2ª curve	39.5	-41.5	40.5	4.5	-9.1	6.8	0.1	-1.5	0.8	2025.4
3ª curve	39.5	-41.5	40.5	4.5	-9.1	6.8	0.1	-1.5	0.8	2025.4
MW2	F_{max} (kN)	F_{min} (kN)	$\lvert F_{ave}$ (kN)$\rvert$	$v_{40\%}F_{max}$ (mm)	$v_{40\%}F_{min}$ (mm)	$v_{40\%}$ (mm)	$v_{10\%}F_{max}$ (mm)	$v_{10\%}F_{min}$ (mm)	$v_{10\%}F_{ave}$ (mm)	k (kN/m)
1ª curve	44.8	-55.1	49.9	9.2	-7.2	8.2	0.5	-1.0	0.8	2011.3
2ª curve	39.3	-41.3	40.3	8.7	-5.0	6.9	0.5	-1.0	0.8	1982.8
3ª curve	39.3	-41.3	40.3	8.7	-5.0	6.9	0.5	-1.0	0.8	1982.8

Figure 14 shows the masonry walls hysteresis cycles along the test. According to equation 2 the damping coefficient in each cycle is obtained. In table 3.4 the energy dissipated in cycles at different levels of deformation is presented. As increase in deformation leads to a higher increase in energy dissipation and less damping associated to damage in the timber beams and in the masonry infill.

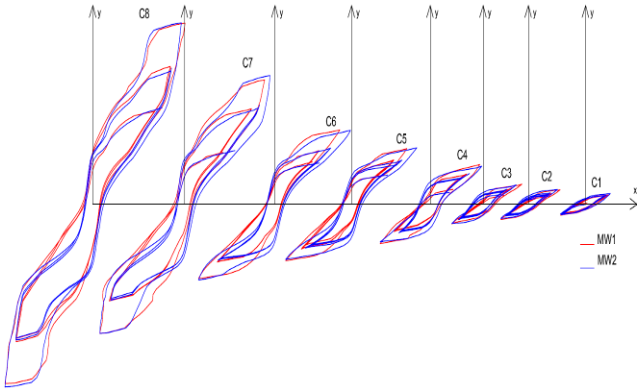

Figure 14. Energy dissipated in each cycle

Table 3.4. Energy dissipated and damping in each cycle

	MW1		MW2	
Nome	Ed (kN/m^2)	ζ (%)	Ed (kN/m^2)	ζ (%)
C1	48,29	17,0	58,45	0,207
C2	69,30	14,3	77,83	0,217
C3	97,74	15,6	114,59	0,173
C4	283,77	16,0	312,95	0,160
C5	416,15	11,3	483,28	0,134
C6	610,34	11,0	652,44	0,119
C7	1377,66	13,0	1406,89	0,131
C8	2043,75	13,2	1984,84	0,127

Figure 15 shows the failure modes of the walls. Rupture in MW1 is associated with compression of the diagonals that caused the shear failure of the intermediate beam. In the case of the model MW2 the wall had an early rupture by cutting parallel of the timber fibres at one end of the intermediate beam.

a)Failure by shear failure of intermediate timber beam for MW1

b) Failure by parallel shear of intermediate timber beam for MW2

Figure 15. Failure mode of masonry wall

4. CONCLUSIONS

The load-displacement diagrams obtained for the timber frames (TF) and masonry walls (MW) are shown in Figure 16. Through the analysis of the behaviour in the load-displacement diagrams, an increase in the wall stiffness for displacements higher than 60 mm was observed, associated with the course limit of the vertical jacks. Due to this behaviour, these values cannot be taken into account for the characterization of the walls. Therefore the analysis is limited to a range of ± 55 mm displacements as shown in Figure 16.

The hysteretic behaviour of the "frontal" wall subjected to cyclic loadings is characterized by nonlinear behaviour, describing the monotonic envelope, with a high ductility response. The maximum strength is 30 kN and 50 kN, for the timber frames and masonry walls respectively,

measured at the displacement of 55 mm which results in a 2.6% drift.

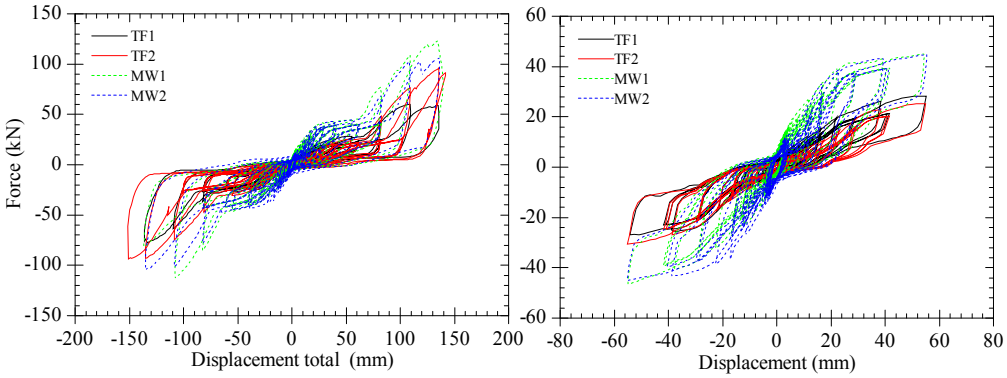

Figure 16. Force-displacement curve

As expected, masonry walls exhibited higher stiffness than timber frames, 2000 kN/m and 600kN/m respectively. Masonry infill is important to the stiffness and especially to the strength of the whole module. The masonry infill also influences the collapse mode, for example by preventing the lateral instability of the compressed diagonal.

The masonry walls also have a greater ability to dissipate energy, which implies a larger damping effect, very relevant regarding the behaviour of the walls subjected to an earthquake loading.

AKCNOWLEDGEMENT

The financial supporte of the Foundation for Science and Technology (FCT) through the research project PTDC/ECM/100168 – REABEPA is acknowledged. The authors also acknowledge HCI for his invaluable help. The laboratory technician Mr. Fernando Alves is also acknowledged for his help in the experimental tests.

REFERENCES

ASTM E2126 – 11. Standard Test Methods for Cyclic (Reversed) Load Test for Shear Resistance of Vertical Elements of the Lateral Force Resisting Systems for Buildings.

Diskaya, H. (2007). Damage Assessment of 19th Century Traditional Timber Framed Structures in Istanbul, From Material to Structure - Mechanical Behaviour and Failures of the Timber Structures, *ICOMOS IWC - XVI International Symposium,* November 2007.

Dogangun A., Tuluk I.O., Livaoglu R., Acar R. (2006). Traditional wooden buildings and their damages during earthquakes in Turkey. *Engineering Failure Analysis* **13**, 981–996

EN 1991-1-1 (2002). Eurocode 1: Actions on structures –part 1-1: General actions – Densities, self-weight. Imposed loads for buildings, commissions of the European Communities (CEN), Brussels, April 2002.

Ferreira, J. G., Teixeira M.J., Dutu, A., Branco, F., Gonçalves, A. (2012). Experimental Evaluation and Numerical Modelling of Timber Framed Walls. *Experimental Techniques*, **Vol.36: 2.**

Gonçalces A, Ferreira J., Guerreiro L, Branco F. (2011). Avaliação Experimental do Comportamento de Paredes de Edificios Pombalinos. *Construlink* **Vol. 9 : 27**.

Gülkan, P., Langenbach, R.(2004). The earthquake resistance of traditional timber and masonry dwellings in Turkey. *13th World Conference on Earthquake Engineering Vancouver, B.C.* **No. 2297.**

ISO 21581 (2010). Timber structures - Static and cyclic lateral load test methods for shear walls. New Delhi: Bureau of Indian Standards.

Krawinkler H., Parisi F., Ibarra L., Ayoub A. and Medina R. (2000). Development of a testing protocol for wood frame structures, Krawinkler. *CUREE-Caltech Woodframe Project Rep.*, Stanford University, Stanford, California.

Langenbach, Randolph (2007). From 'Opus Craticium' to the 'Chicago Frame': Earthquake- Resistant Traditional Construction. *International Journal of Architectural Heritage*, **1: 1**, 29 — 59.

Makarios, T., Demosthenous, M. (2006). Seismic response of traditional buildings of Lefkas Island, Greece. *Engineering Structures* **28**,264–278.

Meireles H.; Bento R.(2010). Cyclic Behaviour of Pombalino Frontal Walls. *Proceedings of the 14th European Conference on Earthquake Engineering (14ECEE)*, Ohrid, F.Y.R.O.Macedonia.

Redondo, E. González, Hernández-Ros, R. Aroca (2003). Wooden framed structures in Madrid domestic architecture of 17th to 19th centuries. *Proceedings of the First International Congress on Construction History* 20th-24th January .